Eur. J. Biochem. **267**, 4583–4592 (2000) © FEBS 2000

Isolation of dermatoxin from frog skin, an antibacterial peptide encoded by a novel member of the dermaseptin genes family

Mohamed Amiche[1], Aurélia A. Seon[1], Henri Wroblewski[2] and Pierre Nicolas[1]

[1]*Laboratoire de Bioactivation des Peptides, Institut Jacques Monod, Paris, France, and* [2] *Groupe 'Membranes et Osmorégulation', UPRES-A CNRS 6026, Université de Rennes, France*

A 32-residue peptide, named dermatoxin, has been extracted from the skin of a single specimen of the tree frog *Phyllomedusa bicolor*, and purified to homogeneity using a four-step protocol. Mass spectral analysis and sequencing of the purified peptide, as well as chemical synthesis and cDNA analysis were consistent with the structure: SLGSFLKGVGTTLASVGKVVSDQF GKLLQAGQ. This peptide proved to be bactericidal towards mollicutes (wall-less eubacteria) and Gram-positive eubacteria, and also, though to a lesser extent, towards Gram-negative eubacteria. Measurement of the bacterial membrane potential revealed that the plasma membrane is the primary target of dermatoxin. Observation of bacterial cells using reflected light fluorescence microscopy after DNA-staining was consistent with a mechanism of cell killing based upon the alteration of membrane permeability rather than membrane solubilization, very likely by forming ion-conducting channels through the plasma membrane. CD spectroscopy and secondary structure predictions indicated that dermatoxin assumes an amphipathic α-helical conformation in low polarity media which mimic the lipophilicity of the membrane of target microorganisms. PCR analysis coupled with cDNA cloning and sequencing revealed that dermatoxin is expressed in the skin, the intestine and the brain. Preprodermatoxin from the brain and the intestine have the same sequence as the skin preproform except for two amino-acid substitutions in the preproregion of the brain precursor. The dermatoxin precursor displayed the characteristic features of preprodermaseptins, a family of peptide precursors found in the skin of *Phyllomedusa* ssp. Precursors of this family have a common N-terminal preproregion followed by markedly different C-terminal domains that give rise to 19–34-residue peptide antibiotics named dermaseptins B and phylloxin, and to the D-amino-acid-containing opioid heptapeptides dermorphins and deltorphins. Because the structures and cidal mechanisms of dermatoxin, dermaseptins B and phylloxin are very different, dermatoxin extends the repertoire of structurally and functionally diverse peptides derived from the rapidly evolving C-terminal domains of precursors of the dermaseptins family.

Keywords: antimicrobial peptide; ceratotoxins; dermaseptins; dermorphin; frog skin

Gene-encoded antimicrobial peptides are an essential defense component of prokaryotic and eukaryotic organisms destined to circumvent invading pathogens and proliferation of commensals microoganisms. Since the discovery in 1970 of bombinin [1], the first gene-encoded peptide antibiotic characterized in eukaryotes, amphibian skin secretions have become important sources of new antimicrobial agents [2–4]. In addition to biologically active peptides which are very similar to mammalian neuropeptides and hormones [5,6], the frog dermatous glands synthesize and store an extraordinarily rich variety of wide-spectrum antimicrobial peptides that are released onto the outer layer of the skin to provide an effective and fast-acting defense against harmful microorganisms. As a rule, a given amphibian species produces a unique repertoire of small peptide antibiotics that have overlapping structural features, but often target specific microorganisms [7]. The simultaneous presence of closely related antimicrobial peptides agents acting in synergy is thought to provide frogs with an extended shield against a wider range of harmful invaders. Furthermore, amphibians belonging to different families, genera and species store distinct set(s) of antimicrobial peptides with differing chain length, charge, hydrophobicity and activity spectrum. The impressive interspecies variations in the expression of skin antimicrobial peptides, which likely result from the coevolution of microorganisms specifically pathogenic for each frog species, may be exploited for discovering new antimicrobial molecules targeting specific microorganisms for which the therapeutic armamentarium is scarce.

To date, the microbicidal peptides of the frog skin have been arranged into three broad families on the basis of their sequence/tridimensionnal fold similarities: (i) linear amphipathic helix-forming peptides such as the magainins from the African clawed frog *Xenopus laevis* [8] and the caerins from the Australian anura *Litoria splendida* [9–11]; (ii) six different groups of disulfide-containing peptides identified in skin of Ranid, namely brevinins-1 and -2, ranaeturins-1 and -2, esculentins-1 and -2 [12–18]; (iii) the temporins, cystine-free hydrophobic peptides isolated from *Rana temporaria,* comprised of only 10–13 residues [19].

In a previous study, we isolated a whole family of antimicrobial peptides, the dermaseptins B, from the skin

Correspondence to P. Nicolas, Laboratoire de Bioactivation des Peptides, Institut Jacques Monod, Université Paris 7, 2 Place Jussieu, 75251 Paris Cedex 05, France. Fax: +33 01 44 27 59 94.
E-mail: pnicolas@ccr.jussieu.fr

Abbreviations: amu, atomic mass units; DAPI, 4′,6-diamidino-2-indole; $diSC_3$-(5), 3,3′-dipropyl-2,2′-thiadicarbocyanine iodide; $\Delta\Psi$, membrane potential; Fmoc, fluoren-9-ylmetoxycarbonyl; HOBt, hydroxybenzotriazol; MIC, minimal inhibitory concentration; MLC, minimal lethal concentration; TFA, trifuoroacetic acid.

(Received 23 March 2000, revised 15 May 2000, accepted 24 May 2000)

secretions of the South American frog *Phyllomedusa bicolor* [20,21]. Dermaseptins B are 24–34 residues long, polycationic (Lys-rich) peptides having a conserved Trp residue at position 3 and a AGK(Q)AA(V)LG consensus motif in the mid-region. Although the six characterized dermaseptins have differing lengths and amino-acid sequences they are all broad-spectrum microbicides that cause the lysis of many bacteria, protozoa, yeasts and fungi, but have no harmful effect on differentiated mammalian cells [20–22]. These peptides owe their cytolytic properties to a predilection to forming cationic amphipathic α-helical structures when associated with lipid membranes [22]. As these peptides kill microorganisms rapidly by destroying their plasma membrane, they are unlikely to induce antibiotic-resistant bacteria [23]. This makes them promising candidates for inclusion in new treatments of nosocomial infections and multidrug-resistant infections. Molecular cloning of the corresponding biosynthetic precursors [21,24,25] unexpectedly revealed that the preproregion of preprodermaseptins B, encompassing a 22-residue signal peptide and a 22–23-residue acidic propiece, is highly conserved and has striking similarities to the corresponding preproregions of the precursors of the dermorphins and deltorphins [26–32], D-amino-acid-containing opioid heptapeptides occuring in the skin of frogs of the family Phyllomedusinae [33–35].

Here we report the discovery of dermatoxin, a novel 32-residue linear antimicrobial peptide, in the skin secretions of *P. bicolor*. Dermatoxin is cationic, amphipathic and membranotropic but cannot be linked to any of the frog skin peptides isolated to date. Meanwhile it is excised from a prepropeptide which exhibits considerable similarity to the preprodermaseptins. Dermatoxin is thus an unexpected addition to the structurally and functionally diverse peptide subfamilies derived from the hypervariable C-terminal domain of precursors of the dermaseptin family.

MATERIALS AND METHODS

Chemicals

9-Fluorenylmethoxycarbonyl (Fmoc) protected L-amino acids and poly(ethylene glycol) poly(styrene)-graft copolymer support (PEG-PS resin, substituted at 0.18 meq·g^{-1}) were from Milligen (Bedford, MA, USA). Chemicals for peptide synthesis [dimethylformamide, dichloromethane, diisopropyl-carbodiimide, hydroxybenzotriazol (HOBt), piperidine, trifluroacetic acid (TFA), acetonitrile] were obtained from commercial sources and were of the highest purity available.

Housing the South American frog, *Phyllomedusa bicolor*

Frogs were housed in large wooden cages (120 × 90 × 90 cm; 12 animals per cage), covered on three sides by plastic mosquito net. *Phyllodendron*, *Potos* and *Dracena* were used as perches, and water bowls were provided for nocturnal baths. The frogs were fed crickets. Relative humidity was maintained at 65% by a constantly operating humidifier. The temperature was maintained at 25 ± 1 °C.

Purification of dermatoxin from frog skin extract

A *P. bicolor* frog was killed and the skin and adherent tissues were minced with scissors and extracted for 1 min using a Braun press in 40 mL 10% acetic acid at 4 °C. The extract was centrifuged twice for 30 min at 10 000 ***g*** and the supernatant lyophilized. The dried extract was dissolved in 200 mL 5% acetic acid and lyophilized (yield = 800 mg). This lyophylisate was subjected to reversed-phase HPLC on a Waters RCM compact preparative cartridge Deltapak C18 (300 Å, 100 × 25 mm) loaded with 40 mg extract in water containing 0.07% TFA. The column was washed for 1 min with 0.07% TFA/water, and the extract was eluted at a flow rate of 8 mL·min^{-1} with a 0–60% linear gradient of acetonitrile containing 0.07% TFA (from 3 to 33 min). Ten-milliliter fractions were collected. Fractions eluting between 26 and 32 min were pooled and fractionated again on the same HPLC column. After an initial 2 min wash in 0.1% TFA/water, elution was achieved with a linear biphasic gradient of 26–41% of acetonitrile for 75 min (0.2% acetonitrile·min^{-1}) and 60% acetonitrile for 5 min, at a flow rate of 1 mL·min^{-1}. Fractions eluting between 78 and 80 min were pooled and fractionated once again on the same HPLC column using a linear gradient of 38–54% acetonitrile for 80 min (0.2% acetonitrile·min^{-1}) at a flow rate of 0.7 mL·min^{-1}.

Amino-acid sequence analysis

The amino-acid sequences were determined on a gas-phase automatic protein sequencer (Applied Biosystems 476A pulsed liquid delivery peptide sequanator). Phenylthiohydantoin amino acids were detected with an on-line Applied Biosystem 120A analyzer. Data were collected and analysed with an Applied Biosystems 900A module calibrated with 32.5 pmol of phenylthiohydantoin amino-acid standards.

Electrospray ionization mass spectrometry

Mass spectral analysis was performed as described previously [36] using a quadrupole coupled electrospray mass spectrometer (VG Platform). The mass scale was calibrated using myoglobin. The accuracy was ± 0.1 atomic mass units (amu). Samples (25 pmol) were dissolved in water/acetonitrile (1 : 1, v/v) containing 0.2% formic acid and introduced via a capillary using a microliter syringe. An electrospray voltage of 5 kV was applied to the internal wall of the source at the origin of the liquid dispersion for electrospray formation and ion extraction. Ions were detected and analyzed in the positive mode on the basis of their *m/z* ratio.

Solid-phase peptide synthesis

Dermatoxin was prepared by stepwise solid-phase synthesis using Fmoc polyamide active ester chemistry on a Milligen 9050 pepsynthesizer. All Nα-Fmoc-amino acids were from Milligen. Side-chain protections were *tert*-butyloxycarbonyl for lysine, *Otert*-butyl ester for aspartic acid, *Otert*-butyl ether for threonine and trityl for glutamine. Synthesis was carried out using a triple-coupling protocol: Nα-Fmoc-amino acids (4.4 molar excess) were coupled for 30–60 min with 0.23 M diisopropylcarbodiimide in a mixture of dimethylformamide and dichloromethane (60 : 40, v/v). Acylation was checked after each coupling step using the Kaiser test. Cleavage of the peptidyl resin and side-chain deprotection were carried out at a concentration of 40 mg of peptidyl resin in 1 mL of a mixture composed of TFA, phenol, thioanisole, water and ethyl methyl sulfide (82.5 : 5 : 5 : 5 : 2.5, v/v/v/v/v) for 2 h at room temperature. After filtering to remove the resin and ether precipitation at −20 °C, the crude peptide was recovered by centrifugation at 5000 ***g*** for 10 min, washed three times with cold ether, dried under nitrogen, dissolved in 20% acetic acid and lyophilized. After lyophilization, the crude peptide was

purified by preparative RP-HPLC on a Waters RCM compact preparative cartridge Deltapak C 18 (300 Å; 25 × 100 mm) eluted at a flow rate of 8 mL·min^{-1} by a multistep linear gradient of acetonitrile in 0.1% TFA in water. The homogeneity of the synthetic peptide was assessed by gas-phase sequence analysis, mass spectrum analysis and analytical HPLC on a Lichrosorb C18 column (5 μm, 4.6 × 250 mm) eluted at a flow rate of 0.75 mL·min^{-1} with a linear gradient of acetonitrile in 0.1% TFA acid/water.

Circular dichroism

Peptide samples were dissolved in water (0.1 mg·mL^{-1}) or in 20 and 30% TFA/water (v/v). CD spectra were recorded on a Jobin-Yvon Mark VI high sensitivity dichrograph linked to a PC microprocessor, at room temperature using a quartz cuvette of 1-mm pathlength. All spectra were recorded with a 1-nm step and were baseline corrected. CD measurements were reported as Δε (M^{-1}.cm^{-1}). The relative helix content was deduced according to Zhong & Johnson [37] as follows:

$$\%\text{helix} = -[\Delta\varepsilon_{222\,\text{nm}} \times 10]/n$$

where $\Delta\varepsilon_{222\,\text{nm}}$ is the CD at 222 nm and n is the number of residues in the peptide. This band is almost exclusively due to the α helix.

Cloning procedure

One adult *P. bicolor* frog was anesthetized with pentobarbital, immersed in liquid nitrogen and kept deep-frozen until further processing. The skin was removed on dry ice and a sample of ≈ 7 g of tissue was homogenized. Total RNAs were extracted as described by Chomczynski & Sacchi [38]. Poly(A$^+$) RNAs were purified over an affinity oligo(dT) spin cellulose column supplied by Pharmacia, and a cDNA library was constructed from skin poly(A$^+$) RNA as described [21] using standard procedures [39]. Recombinant plasmids of the library were extracted from bacteria grown at 37 °C for 16 h in Luria–Bertani medium containing 100 mg·mL^{-1} ampicilin. An aliquot of the cDNA was used for PCR. The reaction was performed using a sense primer T7 (primer T7: 5′-AATAC-GACTCACTATAGGG-3′) and an antisense specific primer corresponding to amino acids 22–28 of dermatoxin (primer 1: 5′-AACAGCTTCCCAAATTGATC-3′) under the following conditions: 94 °C for 240 s, followed by 30 cycles of 94 °C for 40 s, 53 °C for 30 s and 72 °C for 60 s. At the end of the last cycle, the sample was incubated at 72 °C for a further

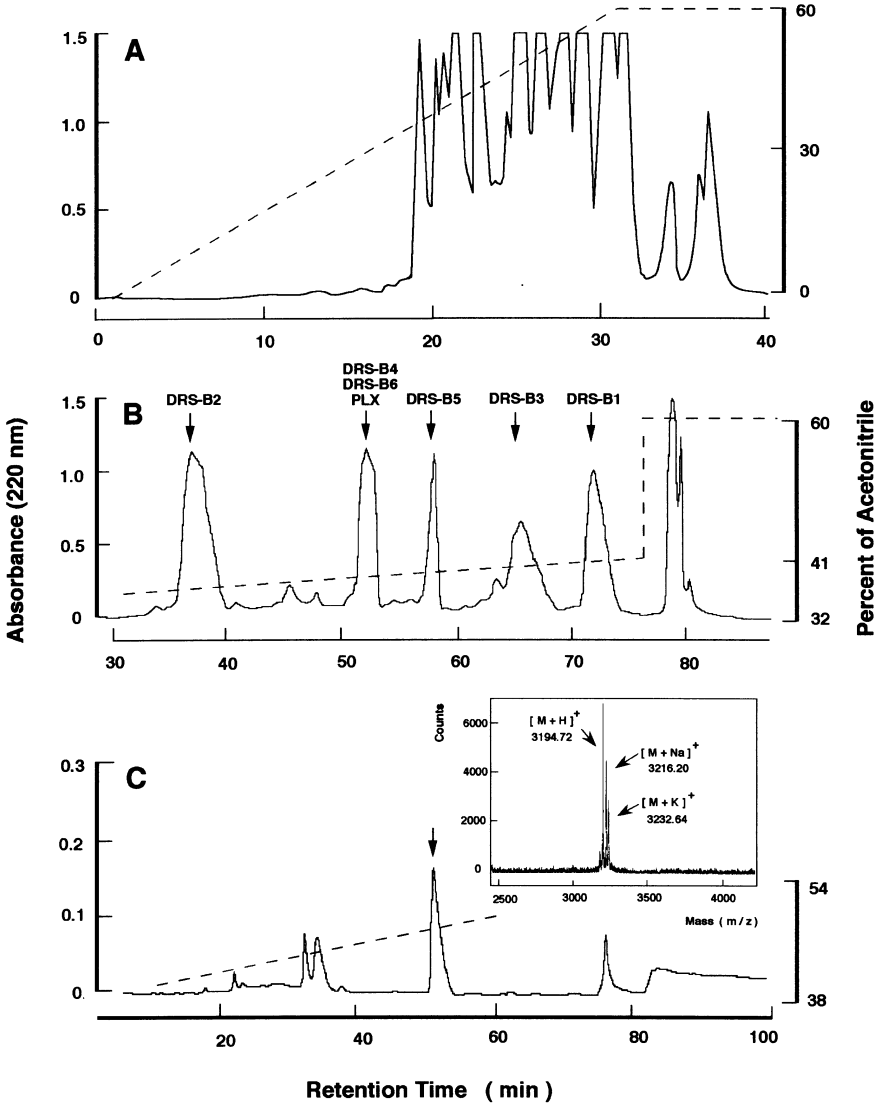

Fig. 1. Purification of dermatoxin from *P. bicolor* skin. (A) Reversed-phase HPLC fractionation of the skin extract on a Waters RCM compact preparative cartridge Deltapak C18 (300 Å, 100 × 25 mm). Elution was carried out at 8 mL·min^{-1} with a 0–60% linear gradient of acetonitrile containing 0.07% trifluoracetic acid. Solid line, absorbance at 220 nm; dashed line, % acetonitrile. (B) HPLC chromatogram of the pooled fractions eluting between 26 and 32 min in Fig. 1A (bars) on the same column. Elution was achieved with a linear biphasic gradient of 26–41% acetonitrile for 75 min and 60% acetonitrile for 5 min, at a flow rate of 1 mL·min^{-1}. Arrows indicate the elution positions of dermaseptin B2 (DRS-B2), dermaseptins B4, B6 and phylloxin (PLX), dermaseptin B5, dermaseptin B3 and dermaseptin B1. (C) Fractions eluting between 78 and 80 min in Fig. 1B were pooled and chromatographed on the same column using a linear gradient of 38–54% acetonitrile for 80 min at 0.7 mL·min^{-1}. Arrow: elution position of synthetic dermatoxin under the same conditions. Inset: Ion spray mass spectrum of purified dermatoxin.

5 min, and electrophoresed in a 1.2% agarose gel. DNA fragments were excised from the gel and purified using the Qiaquick gel extraction kit (Qiagen, France). The PCR product was cloned in the pGEMT-Easy vector system (Promega, France) and sequenced by the dideoxy chain termination technique [40] in double-stranded pGEMT-Easy vector. We used the fluorescence-labeled dye-terminator method and an ABI 377 automatic sequencer. To determine the sequence of the 3′-end of the preprodermatoxin, we used cDNA as a template with an antisense universal primer (primer PU: 5′-GTAAAAC-GACGGCCAGTG-3′) and a 3′-sense gene-specific primer deduced from the 5′-cDNA preprodermatoxin (primer 2 for RACE: 5′-TTGGGGAGCTTTCTAAAAGG-3′; primer 3 for nested PCR: 5′-GTAGGAACCACATTAGCAAG-3′). The temperature cycle used for the RACE PCRs was: 94 °C for 240 s, 30 cycles of denaturation at 94 °C for 40 s, annealing at 55 °C for 30 s and extension at 72 °C for 60 s, and a final extension step of 72 °C for 5 min. PCR products were purified using a Qiaquick Kit, cloned in pGEMT-Easy vector (Promega, France), and sequenced as above.

Tissue distribution

mRNA from frog skin, brain and intestine were prepared using the Micro-FastTrack kit (Invitrogen). RT-PCR were performed using the SuperScript One-Step RT-PCR System (Life Technologies). Both cDNA synthesis and PCR were performed in a single tube using specific primers deduced from the skin preprodermatoxin (primer 4 sense: 5′-CCTTGTAC-TATTCCTTGGATT-3′ and primer 5 antisense: 5′-TATGCTT-TAATATAGTTAGTGC-3′) and mRNA from frog brain, skin or intestine. The following thermal cycle profile was used for the RT-PCR: 45 °C for 30 min then 94 °C for 2 min, followed by 30 cycles of 94 °C for 40 s, 55 °C for 30 s and 72 °C for 60 s, and a final extension step of 72 °C for 5 min. This was followed by nested PCR using sense primer 6: 5′-CTATTCCTTGGATTGGTCTC-3′ and an antisense primer 7: 5′-CCTAAGAGTAATGGGATTTCA-3′. The following thermal cycle profile was used: 94 °C for 240 s, then 72 °C for 1 min followed by 30 cycles of 94 °C for 40 s, 55 °C for 30 s and 72 °C for 5 min. PCR products were purified using a Qiaquick Kit, cloned in pGEMT-Easy vector (Promega) and sequenced as mentioned above.

Antimicrobial assays

Mollicutes (*Acholeplasma laidlawii* A-PG8 and *Spiroplasma melliferum* BC3) were cultured as described previously [41]. Gram-positive eubacteria (*Bacillus megaterium* KM and ATCC 9885, *Staphylococcus aureus* ATCC 25923 and *Corynebacterium glutamicum* ATCC 13032) and Gram-negative eubacteria (*Burkholderia cepacia* ATCC 25416, *Pseudomonas aeruginosa* ATCC 27853, *Sinorhizobium meliloti* 102F34 and *Salmonella typhimurium* CIP 6062) were grown in Luria–Bertani broth at 37 °C. The minimal inhibitory concentrations (MICs) were determined in 96-well microtitration plates by growing the bacteria in the presence of twofold serial dilutions of peptide. The starting cell concentration in each well was of 10^6 c.f.u.·mL^{-1} for mollicutes and 10^5 c.f.u.·mL^{-1} for the other bacteria. To distinguish bacteriostatic effects from bactericidal ones, bacteria were incubated for 2 h in the presence of different concentrations of peptide and plated on solid culture medium containing 1% noble agar. The agar plates were examined daily for the formation of colonies. The minimal lethal concentration (MLC) was defined as the lowest peptide concentration capable of killing ≥ 99% of the cells. All assays were performed in triplicate.

Microscopy

The 4′,6-diamidino-2-phenylindole (DAPI) staining technique [42] was used to assess the presence of DNA within bacteria. Cell suspensions (10^{10} c.f.u.·mL^{-1} of culture medium in the case of *S. melliferum* BC3 and 10^9 c.f.u.·mL^{-1} for *B. megaterium* KM and *C. burkholdreria* ATCC 25416) were treated with different peptide concentrations and subsequently fixed for 2 h with 2.5% glutaraldehyde pH 7.0 at room temperature. After washing with deionized water, the cells were stained for 15 min with 10 μg DAPI·mL^{-1}, washed again in water, spread over a glass slide and observed by reflected light fluorescence

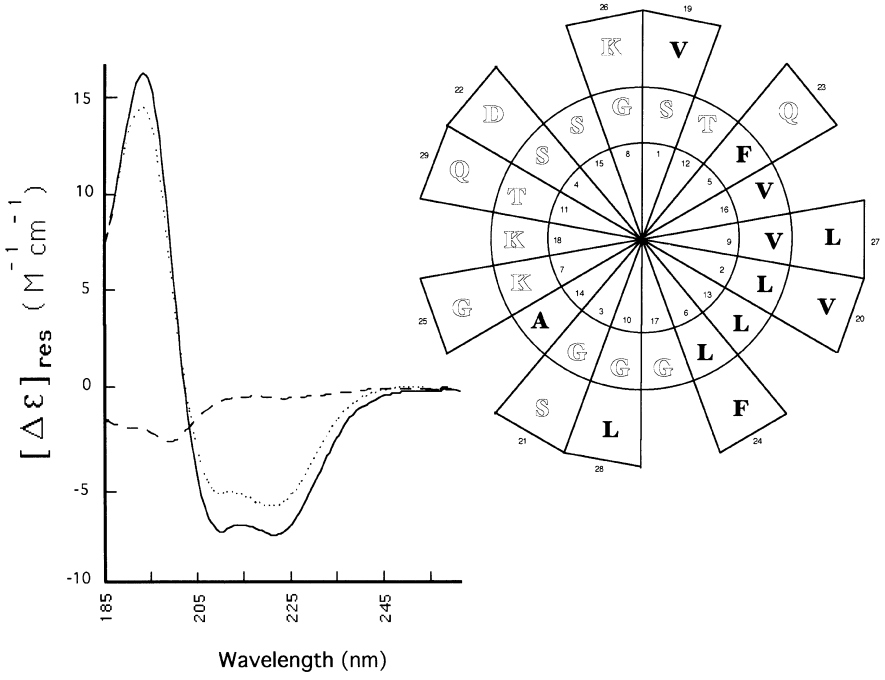

Fig. 2. Secondary structure of dermatoxin. (A) CD spectra of dermatoxin at 20 °C in the presence and abscence of trifluoroethanol. The trifluoroethanol percentages (by volume) used were as follows: 0% (- - -), 20% (……) and 30% (––––). (B) Helical wheel plot of dermatoxin showing its amphipathic structure. In this conformation, periodic variation in the hydrophobicity value of the residues along the peptide backbone with a 3.6 residues per cycle period characterize an α helix [53]. Apolar residues are in bold letters

using a Leica Diaplan microscope, a Leica filter cube D, a 3-Λ-Ploemopak illuminator and a Leitz PL Fluotar oil-immersion objective (×100; numerical aperture = 1.32). Micrographs were taken with a Nikon F-801 camera using Ektachrome 64T color reversal film (ISO 64). For paper printing, the images (green fluorescence signal on dark background) were inverted to yield a dark signal on a clear background.

Measurement of membrane potential in *S. melliferum*

Exponentially growing spiroplasma cells were harvested, washed once in 5 mM Hepes buffer pH 7.0 containing 128 mM NaCl and 50 mM D-glucose, and dispersed into the same buffer to obtain a suspension of 10^9 c.f.u.·mL^{-1} (D_{600} = 0.10, 30 μg of cell protein·mL^{-1}). Membrane potential ($\Delta\Psi$) was measured using the fluorescent potentiometric dye 3,3′-dipropyl-2,2′-thiadicarbocyanine iodide (diSC$_3$-[5]) as described previously [43].

RESULTS

Isolation and purification of dermatoxin

Skin extracts were fractionated by RP-HPLC preparative chromatography using a 0–60% linear gradient of acetonitrile in water (Fig. 1A). Fractions eluting between 26 and 32 min were pooled and then fractionated again by RP-HPLC using a linear biphasic gradient of 26–41% of acetonitrile over 75 min, and 60% acetonitrile over 5 min (Fig. 1B). Peaks eluting at ≈ 37 min (32% acetonitrile), 52 min (35% acetonitrile), 58 min (36% acetonitrile), 66 min (38% acetonitrile) and 72 min (39% acetonitrile) contained dermaseptin B2, dermaseptins B4, B6 and phylloxin [44], dermaseptin B5, dermaseptin B3 and dermaseptin B1, respectively.

We focused our attention on the last peak eluted between 78 and 80 min (Fig. 1B). The corresponding fractions were pooled and fractionated again by RP-HPLC using a linear gradient of 38–54% acetonitrile over 80 min (Fig. 1C). The top of the peak eluting at 52 min (48% acetonitrile) was collected manually and analyzed on a C18 Licrosorb HPLC analytical column (not shown). A single component emerged as a symmetrical sharp peak accounting for > 95% of the eluted UV absorbing material. Inspection of the near-UV spectrum of the peak revealed the absence of the tryptophan residue, characteristic signature of the dermaseptins B. The amount of purified peptide recovered from a single frog specimen was 34 μg. The purified material was directly subjected to amino-acid sequence analysis and mass spectral analysis.

Amino-acid sequence and mass spectrometric analysis

The primary structure of the purified peptide was determined up to residue 32 as SLGSFLKGVGTTLASVGKVVSDQFGKLLQAGQ, by automated Edman degradation of the peptide

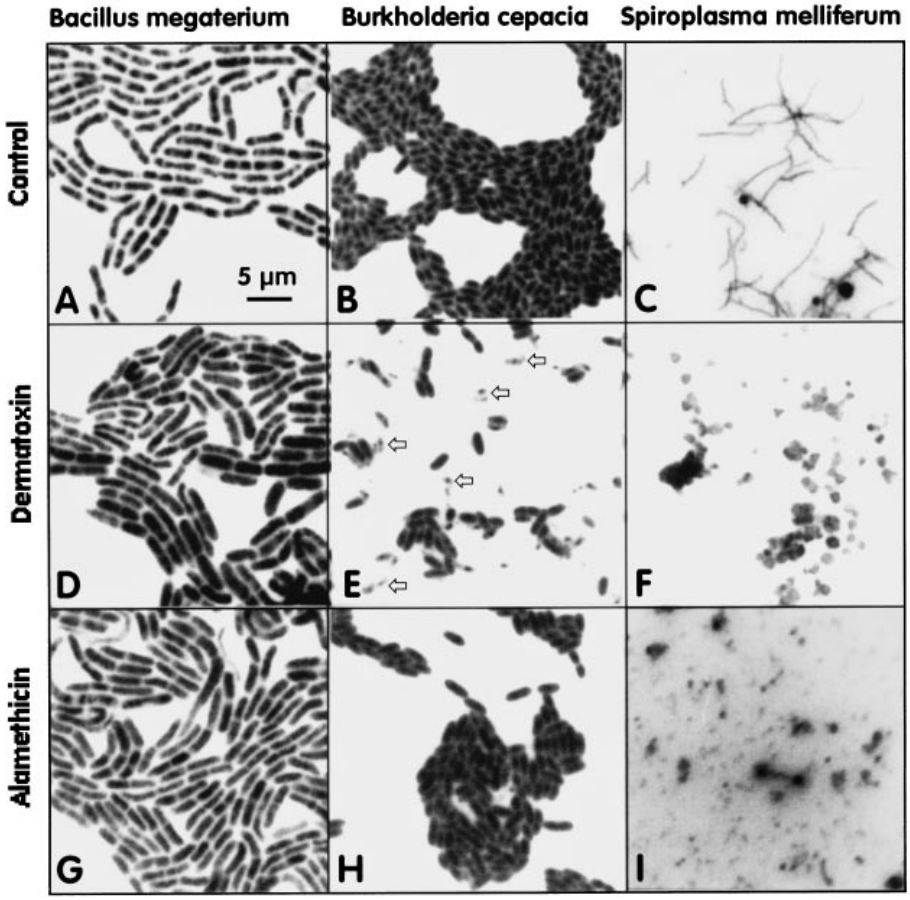

Fig. 3. Fluorescence microscopy of DAPI-stained bacteria. Peptide-treated or untreated cells (controls) were fixed with glutaraldehyde and stained with DAPI for DNA localization. *B. megaterium* KM: control (A) and cells treated for 2 h with 25 μM dermatoxin (D) or 25 μM alamethicin (G). *B. cepacia* ATCC 25416: control (B) and cells treated for 2 h with 50 μM dermatoxin (E) or 50 μM alamethicin (H); broken cells are indicated by arrows. *S. melliferum* BC3: control (C) and cells treated for 1 h with 25 μM dermatoxin (F) or 10 μM alamethicin (I). The recorded images were inverted in order to convert the green fluorescence signal on a dark background to a dark signal on a light background.

Table 1. Antibacterial activity of dermatoxin compared with that of alamethicin.

Strains of bacteria	Dermatoxin		Alamethicin	
	MIC[a]	MLC[b]	MIC[a]	MLC[b]
Mollicutes (wall-less eubacteria):				
Acholeplasma laidlawii A-PG8	12.5	12.5	0.78	1.56
Spiroplasma melliferum BC3	25	50	6.25	6.25
Firmicutes (Gram-positive eubacteria):				
Bacillus megaterium KM	6.25	12.5	3.12	6.25
Bacillus megaterium ATCC 9885	6.25	25	6.25	12.5
Corynebacterium glutamicum ATCC 27853	25	50	3.12	25
Staphylococcus aureus ATCC 25923	R	R	25	100
Gracilicutes (Gram-negative eubacteria):				
Burkholderia cepacia ATCC 25416	R	R [(c)]	R	R
Pseudomonas aeruginosa ATCC 2785	R	R	R	R
Salmonella typhimurium CIP 6062	R	R	R	R
Sinorhizobium meliloti 102F34	25	100	25	R

[a] MIC, minimal peptide concentration (μM) required for total inhibition of cell growth in liquid medium. [b] MLC, minimal peptide concentration (μM) necessary to kill ≥ 99% of the bacteria. Strains were considered resistant (R) when their growth was not inhibited by peptide concentrations up to 100 μM. [c] Between 25 and 100 μM dermatoxin consistently killed ≈ 50% of *B. cepacia* cells.

(100 pmol). Because sequence analysis does not yield information about post-translational modifications of amino-acid side-chains, the purified peptide was also subjected to mass spectral analysis using electrospray ionization spectrometry. An unequivocal pseudomolecular ion was observed that corresponded to a monoprotonated species $[M + H]^+$ whose molecular mass was 3194.72 ± 0.1 Da (Fig. 1, inset). Comparison of the peptide mass calculated from the sequence (3193.76 Da) with the mass of the unprotonated molecule measured by mass spectrometry suggested that we had the full sequence of the molecule and that the peptide is not carboxamidated. The peptide is cationic (pI ≈ 9.7) and rich in Gly (19%), Leu (16%), Ser (12.5%) and Val (12.5%).

Secondary structure of dermatoxin

Secondary structure prediction using a combination [45] of the Hierarchical Neural Network, Predator (incorporation of nonlocal interactions in protein secondary structure prediction), self-optimized method for protein secondary structure prediction (SOPM) and SIMPA (algorithm for secondary structure determination in protein based on sequence similarity) methods indicated that dermatoxin has an overall propensity to assume an α-helical conformation encompassing residues 1–29. Figure 2A shows the far-UV CD spectra of dermatoxin in the absence and presence of trifluoroethanol. The far-UV CD spectra of dermatoxin in aqueous solution displayed a weak minimum at 225 nm and a strong minimum at 200 nm. The presence of a strong minimum at 200 nm reflects the large degree of unordered structure, while the weak minimum at 225 nm could signify the existence of either a very weak amount of α helix or a mixture of nascent 3_{10} helix and α helix [46]. As shown in Fig. 2, addition of small amounts of trifluoroethanol to the aqueous solution of dermatoxin strongly modifies the dichroic spectra. Ellipticity decreased at both 208 and 222 nm and increased at 190 nm, depicting stabilization of the α helix structure (75% α helix content in 30% trifluoroethanol) over the random structure. When plotted on a Schiffer-Edmunson α-helical wheel (Fig. 2B), dermatoxin-[1–29] had a well-behaved amphipathic helical structure, i.e. almost all of the charged and polar residues were aligned on a portion of the helical cylinder and the lipophilic side chains occupy the remaining surface.

Solid-phase synthesis of dermatoxin

Dermatoxin was synthesized using the solid-phase method to confirm the proposed structure and demonstrate that the biological activities of the native peptide reflect its intrinsic properties. Purification of the synthetic peptides was performed by RP-HPLC. The purified synthetic material had the chemical and physical criteria of dermatoxin, and was indistinguishable from the natural product. Analytical HPLC analysis revealed that synthetic dermatoxin eluted at exactly the same position as the natural substance, and coinjection of the native and synthetic peptides gave a single symmetrical peak (not shown); the sequences of synthetic dermatoxin were determined up to Gln32 using automated Edman degradation; mass spectrometry of a sample of the synthetic peptide gave a pseudo-molecular ion at an *m/z*-value corresponding to a species with a molecular mass identical to that of the natural peptide. Because the synthetic product was indistinguishable from its natural counterpart, it was used in the following to evaluate the antimicrobial activity.

Antimicrobial activities

Synthetic dermatoxin was tested for antibacterial activity against 10 strains of bacteria including the two mollicutes (wall-less bacteria) *A. laidlawii* and *S. melliferum*, the three Gram-positive bacteria *B. megaterium* (two strains), *C. glutamicum* and *S. aureus*, and the four Gram-negative bacteria *B. cepacia*, *P. aeruginosa*, *S. typhimurium* and *S. meliloti*. These bacteria also differ in their biotopes which contribute to the diversity of the chosen panel. *A. laidlawii* is a vertebrate parasite which frequently contaminates human and animal tissue cell cultures. *B. cepacia*, *P. aeruginosa* and *S. aureus* are opportunitsic human pathogens, while *S. melliferurm* is a

```
Skin        AGAACTACTCTGTGGCATTCTGTCCTCCAGAACTCTCTGAATTACAAGAGCAGAC  55

                1                   5                  10
                M   A   F   L   K   K   S   L   F   L   V   L   F   L
Skin        ATG GCT TTC CTG AAG AAA TCT CTC TTC CTT GTA CTG TTC CTT  97
               15                  20                  25
                G   L   V   P   L   S  L(I) C   E  S(E) E   K   R   E
Skin        GGA TTA GTC CCC CTT TCC CTC TGT GAA AGC GAG AAA AGA GAA  139
Intestine                   --- --- --- --- --G --- --- --- --- ---
Brain                       --- --T A-- --C --- GAA --- --- --- ---
                    30                  35                  40
                 G   E   N   E   E   E   Q   E   D   D   Q   S   E   E
Skin        GGG GAA AAT GAG GAA GAA CAA GAG GAC GAT CAA AGT GAG GAG 181
Intestine   --- --- --- --- --- --- --- --- --- --- --- --- --- ---
Brain       --- --- --- --- --- --- --- --- --- --- --- --- --- ---
                        45                  50                  55
                 K   R   S   L   G   S   F   L   K   G   V   G   T   T
Skin        AAG AGA AGC TTG GGG AGC TTT CTA AAA GGT GTA GGA ACC ACA 223
Intestine   --- --- --- --- --- --- --- --- --G --- --- --- --- ---
Brain       --- --- --- --- --- --- --- --- --- --- --- --- --- ---
                            60                  65                  70
                 L   A   S   V   G   K   V   V   S   D   Q   F   G   K
Skin        TTA GCA AGT GTA GGA AAA GTG GTT TCA GAT CAA TTT GGC AAG 265
Intestine   --- --- --- --- --- --- --- --- --- --- --- --- --- ---
Brain       --- --- --- --- --- --- --- --- --- --- --- --- --- ---
                                75
                 L   L   Q   A   G   Q   G   *
Skin        CTG CTC CAA GCA GGT CAA GGC TAAAAAAAAATTGAAATCCCATTACTC 313
Intestine   --- --- --- --- --- --- --- --- --- ---
Brain       --- --- --- --- --- --- --- --- --- ---

Skin        TTAGGAGCACTAACTATATTAAAGCATATTAAACAC (Poly A)            349
```

Fig. 4. Nucleic acid and deduced amino-acid sequences of cDNAs encoding dermatoxin from the skin, brain and intestine of *P. bicolor*. The predicted amino-acid sequence of preprodermatoxin is given in capital letters above the nucleotide sequence. Numbers on the right indicate the positions of the nucleotides and amino acids. Nucleotides are numbered positive from the 5′ to 3′-ends of the cDNAs. Amino acids are numbered starting with position 1 in the ORFs. Amino acids in parentheses correspond to changes in the brain dermatoxin sequene compared with that of the skin. The amino-acid sequence of dermatoxin is given in bold. A solid line is drawn under the amino-acid sequence of the signal peptide.

honeybee pathogen. The other bacteria are nonpathogenic, with *B. megaterium* and *S. meliloti* being soil bacteria, and *C. glutamicum* being used in the industrial production of glutamic acid. As shown in Table 1, dermatoxin inhibited the growth of six of 10 strains, with a greater efficacy against mollicutes and Gram-positive bacteria. Dermatoxin proved to be bactericidal with MLCs (12.5–100 μM) most often equal to twice the corresponding MICs (6.25–25 μM). The antibacterial spectrum of dermatoxin was similar to that of the peptaibol alamethicin, a 20-residue peptaibol (i.e. a peptide containing α-methyl-alanines) produced by soil fungi such as *Trichoderma viride*. Alamethicin is well characterized at the structural and functional levels [47,48] and probably forms voltage-dependent chanels in bacterial target membranes similar to those observed in model membranes [49]. It thus appears convenient to use alamethicin as a reference for the characterization of new membrane-active peptides. Alamethicin is generally more efficient than dermatoxin, but it should be noted that 25–100 μM dermatoxin was capable of killing 50% of *B. cepacia* cells whereas alamethicin was inactive even at a concentration of 100 μM.

Observation of the cells using reflected light fluorescence microscopy after DNA-staining with DAPI revealed three distinct situations with respect to the morphological effects of dermatoxin (Fig. 3). *B. megaterium* did not show any visible alteration after a 2-h treatment with 25 μM dermatoxin or alamethicin (compare Fig. 3A,D,G). Alamethicin-treated *B. cepacia* cells (Fig. 3H) were not different from untreated cells (Fig. 3B), whereas ≈ 50% of the cells were damaged by 50 μM dermatoxin (Fig. 3E). In *S. melliferum*, a bacterium which is not protected by a cell wall, the effects were more dramatic. After 1 h of treatment with 25 μM dermatoxin, the filamentous, helical cells (Fig. 3*C*) were split into coccoid vesicles still containing DNA (Fig. 3F), whereas 10 μM alamethicin split the cells into much smaller vesicles (Fig. 3I). The low DAPI-staining of these vesicles and the observation of background fluorescence in this latter case suggest that alamethicin effectively lysed the cells, releasing DNA into the medium. The effects of the peptides on the morphology of spiroplasma cells proved to be correlated with their effects on the membrane potential of nongrowing cells: 2.5 μM dermatoxin decreased within 3 min the potential from ≈ 68 to 38 mV

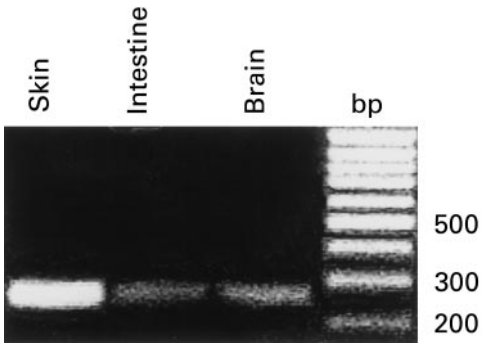

Fig. 5. Tissue distribution of mRNA for preprodermatoxin. Amplification products generated by RT-PCR from frog skin, brain and intestine mRNAs were electrophorezed in 1.2% agarose gel.

```
                                  *
DRT       MAFLKKSLFLVLFLGLVPLSLCESEKREGENEEEQEDD-Q---SEEKR SLGSFLKGVGTTLASVGKVVSDQFGKLLQAGQG
DRS-B1    MDILKKSLFLVLFLGLVSLSICEEEKRENEDEEKQ-DDEQ---SEMKR AMWKDVLKKIGTVALHAGKAALGAVADTISQGEQ
DRS-B2    MAFLKKSLFLVLFLGLVSLSICEEEKRENEDEEEQEDDEQ---SEMKR GLWSKIKEVGKEAKAAAKAAGKAALGAVSEAVGEQ
DRS-B3    MAFLKKSVFLVLFLGLVSLSICEEEKREEENEEKQEDDEQ---SEEKR ALWKNMLKGIGKLAGQAALGAVKTLVGAE
DRS-B4    MAFLKKSLFLVLFLGLVSLSICEEEKRENKDEIEQEDDEQ---SEEKR ALWKDILKNVGKAAGKAVLNTVTDMVNQGEQ
DRS-B6    MAFLKKSLFLVLFLGLVSLSVCEEEKRENEDEMEQEDDEQ---SEEKR ALWKDILKNAGKAALNEINQLVNQGEL
PLX       MVFLKKSLLLVLFVGLVSLSICEENKREEHEEIE-ENKEK---AEEKR GWMSKIASGIGTFLSGIQQG
DRM       MSFLKKSLLLILFLGLVSLSVCKEEKRETEEENENEE-NHEEGSEMKR YAFGYPSGEA
DELT      MSFLKKSLLLVLFLGLVSHSVCKEEKRETEEENENEEENHEVGSEMKR YMFDLMDGEA
DELT II   MSFLKKSLLLVLFLGLVSHSVCKEEKRETEEENENEEENHEVGSEMKR YAFWYPN
```

Fig. 6. Comparison of preprodermatoxin to some of the proforms belonging to the dermaseptins family of peptide precursors. Alignment of the predicted amino-acid sequences of preprodermatoxin (DRT), preprodermaseptins B1, B2, B3, B4 and B6 (DRS) [21,24,25], preprophylloxin (PLX) [44], preprodermorphin (DRM) [27], preprodeltorphins (DELT) [31] and preprodeltorphin II (DELT-II) [32] from *Phyllomedusa* ssp. Gaps (–) have been introduced to maximize sequence similarities. The signal peptide (residues 1–22), the acidic propiece and the processing site Lys-Arg are given in bold. The star indicates the putative cleavage site of the signal peptide. Sequences corresponding to the mature peptides are given in italics.

(inside negative), whereas under the same conditions, the potential was fully collapsed by 2.5 μM alamethicin.

Cloning of cDNA encoding dermatoxin precursor

We used a PCR amplify the mature preprosequence from skin poly(A^+) mRNA with primers based on the N-terminal and C-terminal coding sequences of dermatoxin. Because PCR experiments provided only partial informations about the target sequence, the cDNA ends were amplified on plasmids prepared from the cDNA library. A cloned 349-bp cDNA was obtained and contained an ORF encoding a 77 amino-acid sequence starting with a methionine codon and ending with a stop codon (Fig. 4). The deduced amino-acid sequence begins with a 22-residue putative signal peptide containing numerous hydrophobic amino-acid residues. The cleavage site for the signal peptidase is most likely located after the cysteine residue in position 22 as predicted by the method of Von Heijne [50]. The putative signal sequence (residues 1–22) is followed by an acidic propiece (residues 23–44) comprising 22 residues with a pair of basic residues Lys43-Arg44 at its C-terminus. The dermatoxin progenitor sequence is located at the extreme C-terminus of the precursor, flanked to the acidic propiece. Cleavage of the precursor at the carboxyl side of the basic doublet by endoproteases and removal of the basic residues by carboxypeptidases would also liberate, on addition to the 32-residue dermatoxin, an acidic peptide of 20 residues with unknown activity, which is extremely rich in glutamic acid (45%, normal 6.2%).

The cDNA sequence clearly confirmed the amino-acid sequence of dermatoxin obtained using biochemical methods and showed that the extra Gly residue at the carboxyl end of the dermatoxin progenitor sequence is not involved in the formation of a C-terminal peptide amide. Preprodermatoxin also had the characteristic features of the preproforms that belong to the dermaseptin family of peptide precursors, including a conserved signal peptide and an acidic propiece followed by a typical Lys-Arg processing site. The preproregion of preprodermatoxin is superimposable on that of other precursors of this familly with only a few exceptions (Fig. 6). It is thus likely that preprodermatoxin is a hitherto unknown member of the dermaseptins family of peptide precursors.

Tissue distribution of preprodermatoxin

The distribution of mRNA for preprodermatoxin was examined by RT-PCR using specific oligonucleotide primers (see Matertials and methods). A single amplification signal was observed at the expected size in the skin, intestine and brain (Fig. 5). To certify that the amplified products correspond to preprodermatoxin mRNA, the purified PCR products were cloned in pGEM-Easy vector and sequenced. As shown in Fig. 4, isolated clones from the intestine and brain have the same sequence as the skin preprodermatoxin except for two neutral base changes in the translated region of the former, and six nucleotide changes in the latter which cause a Ile21 for Leu21 and Glu24 for Ser24 substitution in the preproregion of the brain precursor. Variation between the brain, skin and gut cDNA nucleotide sequences suggest that there may be additional alleles or more than one dermatoxin gene.

DISCUSSION

Here we report the isolation of dermatoxin, a novel 32-residue linear peptide with bactericidal activity, in skin secretions of *P. bicolor* Dermatoxin is made as a preproprotein that belongs to the dermaseptin family of peptide precursors which are characterized by strongly conserved preproregions followed by strikingly variable C-terminal sequences corresponding to chemically and functionally different mature peptides. They include the dermaseptins B and phylloxin [44], amphipathic antimicrobial peptides from *Phyllomedusa* ssp., as well as dermorphins and deltorphins, D-amino-acid-containing heptapeptides which are very potent and specific agonists of the μ-opiod or δ-opioid receptors [33–35]. Dermatoxin is both amphipathic and bactericidal but its sequence and mechanism of cell killing are very different to those of dermaseptins B and phylloxin. Yet, the preproregion of preprodermatoxin is superimposable on that of preprodermaseptins B with only few exceptions (Fig. 6), i.e. the amino-acid positional identity between the N-terminal regions encompassing the signal peptides and the acidic propiece is $>80\%$ in the peptide sequences. Also, the 5′-UTR and 3′-UTR of the corresponding cDNAs share 45–86% and 47–57% identity, respectively, in the regions of overlap. A similar conclusion can be drawn when preprodermatoxin is compared with other members of the preprodermaseptin family (Fig. 6). The skin of these frogs thus seems to contain a whole family of transcribed genes which have a common origin but give rise to peptides with very different primary structures and activities.

Dermatoxin proved to be bactericidal, with a spectrum rather similar to that of alamethicin (Table 1). The two peptides were indeed more active against mollicutes and Gram-positive bacteria than towards Gram-negative bacteria, although

alameticin is more hydrophobic and less amphipathic than dermatoxin. Because only Gram-negative eubacteria are protected by an outer membrane, it is tempting to speculate that their higher resistance to the peptides was due, at least in part, to the presence of this second membrane in their envelope. However, it should be noted that the growth of *S. meliloti* (a Gram-negative bacterium) was inhibited by both peptides and, furthermore, dermatoxin killed ≈ 50% of *B. cepacia* cells (also a Gram-negative bacterium) under conditions in which, as expected, alamethicin was inactive. This observation is important for it shows that *B. cepacia* cell populations contain a mixture of dermatoxin-sentive and unsensitive variants, and that the growth inhibition test in liquid medium fails to reveal such a phenomenon. Further investigation is necessary to determine whether this resistance is specific of the *B. cepacia*/dermatoxin interaction or if it may occur with other antimicrobial peptides and/or with other bacterial species.

Experiments performed with the mollicute *S. melliferum* suggest that the plasma membrane is the primary target of dermatoxin because the peptide depolarized the membrane potential, albeit less efficiently than alamethicin. This interpretation in consistent with the fact that in growth inhibition assays, alamethicin had a higher toxicity towards spiroplasma cells than dermatoxin. Furthermore, the absence of visible alterations of the morphology of *B. megaterium* which, as a Gram-positive eubacterium, is surrounded by a thick cell wall, is also consistent with a mechanism of cell killing based upon the alteration of membrane permeability rather than membrane solubilization as observed with dermaseptins B. We have recently shown that alamethicin collapses the bacterial membrane potential very likely by forming ion-conducting channels through the plasma membrane [49]. It remains, however, to be proven whether this is also the case for dermatoxin. Finally, as regards to antimicrobial activity, the biological significance of the presence of a complex mixture of peptide antibiotics which exhibit significant differences in specificity and potency in *Phyllomedusa* skin may be that they provide the frog with greater protection against a wider range of potential invaders at a minimum metabolic cost.

The conservation of the signal peptide among precursors of the dermaseptin family that encode peptides whose structures and activities diverge widely is a unique phenomenon. Indeed, although the overall organization of eukaryotic signal peptides is evolutionarily conserved, no sequence similarity exists apart from a few exceptions. In mammals for instance, several antimicrobial peptides are issued from the C-terminal variable domain of cathelicidins, a family of precursors that possesses very similar preproregions [51]. However, although the mature peptides differ in their structure and length, they all have similar biological activity. Hence, the evolutionary pressure which results in the conservation of the signal peptide in precursors of the dermaseptin family suggests that this topogenic sequence may have additional functions that remain to be discovered. Along these lines, several mechanisms may contribute to the generation of precursors containing conserved preproregions and multiple forms of mature active peptides. Several genes encoding dermaseptins B have recently been cloned [52] which show a two exon-coding structure, the first containing codons for the conserved 22-residue signal peptide and the first three glutamic residues of the acidic propiece, and the second exon encoding the remainder of the conserved acidic propiece plus the processing signal Lys-Arg and a dermaseptin B progenitor sequence. The small intron that interrupts the two coding exons exhibit strong sequence conservation in all the dermaseptin genes, suggesting that gene family expansion may have occurred recently, or that specific gene conversion events have occurred to ensure overall sequence conservation. Because the conserved preproregion is in the same gene as the mature peptide it cannot have been added on by post-transcriptional events. Also, several mismatches in the 5′-regions of the corresponding cDNAs indicate that, in general, preprodermaseptins do not originate by post-transcriptional processing. If the dermaseptin B genes are representative of other dermaseptin-asociated peptide genes, this organization would favor recombinations involving association of diverse coding exon 2s with the first highly conserved coding exon. Also, frame shift mutations could explain the variations in exon 2 while conservation in the intron sequence could indicate an exon shuffling.

ACKNOWLEDGEMENTS

The expert technical assistance of J.J. Montagne and M.-M. Guéguen is gratefully acknowledged. We thank Monique Monnot for circular dichroism spectroscopy analysis and Ran Nir-Paz for useful suggestions. This work was partly supported by the 'Programme de Recherche Fondamentale en Microbiologie et Maladies Infectieuses et Parasitaires (PRFMMIP)' and the Langlois Foundation (Rennes).

REFERENCES

1. Csordas, A. & Michl, H. (1969) Primary structure of two oligopeptides of the toxin of *Bombina variegata*. *Toxicon* **7**, 103–108.
2. Tossi, A. A data base which more than 400 entries. http://www.bbcm.univ.trieste.it/~tossi/search.html.
3. Nicolas, P. & Mor, A. (1995) Peptides as weapons against microorganisms in the chemical defense system of vertebrates. *Annu. Rev. Microbiol.* **49**, 277–304.
4. Simmaco, M., Mignogna, G. & Barra, D. (1998) Antimicrobial peptides from amphibian skin: what do they tell us? *Biopolymers* **47**, 435–450.
5. Lazarus, L.H. & Attila, M. (1993) The toad, ugly and venomous, wears yet a precious jewel in his skin. *Prog. Neurobiol.* **41**, 473–493.
6. Erspamer, V. (1994) The integument. In *Amphibian Biology*, Vol. 1 (H. Heatwole, ed.), pp. 178–350. Surrey, Beatty and Sons, Chipping Norton, Australia.
7. Mor, A., Hani, K. & Nicolas, P. (1994) The vertebrate peptide antibiotics dermaseptins have overlapping structural features but target specific microorganisms. *J. Biol. Chem.* **269**, 1934–1939.
8. Soravia, E., Martini, G. & Zasloff, M. (1988) Antimicrobial properties of peptides from *Xenopus* granular gland secretions. *FEBS Lett.* **228**, 337–340.
9. Stone, D.J.M., Bowie, J.H., Tyler, M.J. & Wallace, J.C. (1992) The structure of caerin 1-l, a novel antibiotic peptide from Australian tree frogs. *J. Chem. Soc. Chem. Commun.* **17**, 1224–1225.
10. Stone, D.J.M., Waugh, R.J., Bowie, J.H., Wallace, J.C. & Tyler, M.J. (1992) Peptides from Australian frogs. Structure of the caerins and caeridin-1 from *Litonia splendida*. *J. Chem. Soc. Perkin Trans.* **1**, 3173–3179.
11. Wabnitz, P.A., Bowie, J.H. & Tyler, M.J. (1999) Differences in the skin peptides of the male and female Australian tree frog. *Eur. J. Biochem.* **267**, 269–275.
12. Morikawa, N., Hagiwara, K. & Nakajima, T. (1992) Brevinin-1 and -2, unique antimicrobial peptides from the skin of the frog, *Rana brevipoda porsa*. *Biochem. Biophys. Res. Commun.* **189**, 184–189.
13. Simmaco, M., Mignogna, G., Barra, D. & Bossa, F. (1994) Antimicrobial peptides from skin secretions of *Rana esculenta*. Molecular cloning of cDNAs encoding esculentin and brevinins and isolation of new active peptides. *J. Biol. Chem.* **269**, 11956–11961.
14. Clark, D.P., Durell, S., Maloy, W.L. & Zasloff, M. (1994) Ranalexin. A novel antimicrobial peptide from bullfrog (*Rana catesbeiana*) skin, structurally related to the bacterial antibiotic, polymyxin. *J. Biol. Chem.* **269**, 10849–10854.

15. Park, J.M., Jung, J.E. & Lee, B.J. (1994) Antimicrobial peptides from the skin of a Korean frog, *Rana rugosa*. *Biochem. Biophys. Res. Commun.* **205**, 948–952.
16. Park, J.M., Lee, J.Y., Moon, H.M. & Lee, B.J. (1995) Molecular cloning of cDNAs encoding precursors of frog skin antimicrobial peptides from *Rana rugosa*. *Biochim. Biophys. Acta* **1264**, 23–28.
17. Suzuki, S., Olic, Y., Okubo, T., Kakegawa, T. & Tatemoto, K. (1995) Isolation and characterization of novel antimicrobial peptides, rugosins A, B and C, from the skin of the frog, *Rana rugosa*. *Biochem. Biophys. Res. Commun.* **212**, 249–254.
18. Goraya, J., Knoop, F.C. & Conlon, J.M. (1998) Ranatuerins: antimicrobial peptides isolated from the skin of the American bullfrog, *Rana castesbetana*. *Biochem. Biophys. Res. Commun.* **250**, 589–592.
19. Simmaco, M., Mignogna, G., Cannofeni, S., Miele, R., Mangoni, M.L. & Barra, D. (1996) Temporins, antimicrobial peptides from the European red frog *Rana temporaria*. *Eur. J. Biochem.* **242**, 788–794.
20. Mor, A., Amiche, M. & Nicolas, P. (1994) Structure, synthesis and activity of dermaseptin B. *Biochemistry* **33**, 6642–6647.
21. Charpentier, S., Amiche, M., Mester, Y., Vouille, V., Le Caer, J.P., Nicolas, P. & Delfour, A. (1998) Structure, synthesis and molecular cloning of dermaseptins B, a family of skin peptide antibiotics. *J. Biol. Chem.* **273**, 14690–14696.
22. Strahilevitz, J., Mor, A., Nicolas, P. & Shai, Y. (1994) Spectrum of antimicrobial activity and assembly of dermaseptin B and its precursor form in phospholipid membranes. *Biochemistry* **33**, 10951–10960.
23. Shai, Y. (1995) Molecular recognition between membrane-spanning polypeptides. *Trends Biochem. Sci.* **20**, 460–464.
24. Amiche, M., Ducancel, F., Lajeunesse, E., Boulain, J.C., Menez, A. & Nicolas, P. (1993) Cloning of the adenoregulin precursor: relationships with dermaseptin. *Biochem. Biophys. Res. Commun.* **191**, 983–990.
25. Amiche, M., Ducancel, F., Mor, A., Boulain, J.C., Menez, A. & Nicolas, P. (1994) Precursors of vertebrate peptide antibiotics dermaseptin B and adenoregulin have extensive sequence identities with precursors of opioid peptides dermorphin, dermenkephalin and deltorphins. *J. Biol. Chem.* **269**, 17847–17853.
26. Montecucchi, P.C., de Castiglione, R., Piani, S., Gozzini, L. & Erspamer, V. (1981) Amino acid composition and sequence of dermorphin. A novel opiate-like peptide from the skin of *Phyllomedusa sauvagei*. *Int. J. Peptide Protein Res.* **17**, 275–283.
27. Richter, K., Egger, R. & Kreil, G. (1987) D-Alanine in the frog skin peptide is derived from L-alanine in the precursors. *Science* **238**, 200–202.
28. Lazarus, L.H., Wilson, W.E., De Castiglione, R. & Guglietta, A. (1989) Dermorphin gene sequence peptide with high affinity and selectivity for delta opioid receptors. *J. Biol. Chem.* **264**, 3047–3050.
29. Mor, A., Delfour, A., Sagan, S., Amiche, M., Pradelles, P., Rossier, J. & Nicolas, P. (1989) Isolation of dermenkephalin from amphibian skin, a high affinity delta selective opioid heptapeptide containing a D-amino acid residue. *FEBS Lett.* **255**, 269–274.
30. Kreil, G., Barra, D., Simmaco, M., Erspamer, V., Erspamer, G.F., Negri, L., Severini, C. & Corsi, R.P. (1989) Deltorphin, a novel amphibian skin peptide with high selectivity and affinity for delta opioid receptors. *Eur. J. Pharmacol.* **162**, 123–128.
31. Erspamer, V., Melchiorri, P., Falconieri-Erspamer, G., Negri, L., Corsi, R., Severini, C., Barra, D., Simmaco, M. & Kreil, G. (1989) Deltorphins: a family of naturally occuring peptides with high affinity and selectivity for the delta opioid binding sites. *Proc. Natl Acad. Sci. USA* **86**, 5188–5192.
32. Richter, K., Egger, R., Negri, L., Severini, C. & Kreil, G. (1990) cDNAs encoding (D-Ala^2) deltorphin precursors from skin of Phyllomedusa bicolor also contain genetic information for 3 dermorphin-related opioid peptides. *Proc. Natl Acad. Sci. USA* **87**, 4836–4839.
33. Erspamer, V. (1992) The opioid peptides of the amphibian skin. *Int. J. Devl. Neurosci.* **10**, 3–30.
34. Lazarus, L.H., Bryant, S.D., Cooper, P.S. & Salvadori, S. (1999) What peptides these deltorphins be. *Prog. Neurobiol.* **57**, 377–420.
35. Amiche, M., Delfour, A. & Nicolas, P. (1998) Opioid peptides from frog skin. In *d-Aminoacids in Sequence of Secreted Peptides of Multicellular Organisms* (Jollès, P., ed.), pp. 57–71. Birkhäuser Verlag, Basel, Switzerland.
36. Fleury, Y., Dayem, M.A., Montagne, J.J., Chaboisseau, E., Le Caer, J.P., Nicolas, P. & Delfour, A. (1996) Covalent structure, synthesis, and structure–function studies of mesentericin Y105 (37), a defensive peptide from gram-positive bacteria *Leuconostoc mesenteroides*. *J. Biol. Chem.* **271**, 14421–14429.
37. Zhong, L., Johnson, W.C. & Jr0. (1992) Environment affects amino acid preference for secondary structure. *Proc. Natl Acad. Sci. USA* **89**, 4462–4465.
38. Chomczynski, P. & Sacchi, N. (1987) Single-step method of RNA isolation by acid guanidinium thiocyanate–phenol–chloroform extraction. *Anal. Biochem.* **162**, 156–159.
39. Sambrook, J., Fritsch, E.F. & Maniatis, T. (1989) *Molecular Cloning. A Laboratory Manual*, 2nd edn. Cold Spring Harbor Laboratory, Cold Spring Harbor, NY.
40. Sanger, F., Nicklen, S. & Coulson, A.R. (1977) DNA sequencing with chain-terminating inhibitors. *Proc. Natl Acad. Sci. USA* **74**, 5463–5467.
41. Béven, L. & Wroblewski, H. (1997) Effect of natural amphipathic peptides on viability, membrane potential, cell shape and motility of mollicutes. *Res. Microbiol.* **148**, 163–175.
42. Russell, W.C., Newman, C. & Williamson, D.H. (1975) A simple cytochemical technique for demonstration of DNA in cells infected with mycoplasmas and viruses. *Nature* **253**, 461–462.
43. Béven, L., Duval, D., Rebuffat, S., Riddell, F.G., Bodo, B. & Wróblewski, H. (1998) Membrane permeabilisation and antimycoplasmic activity of the 18-residue peptaibols, trichorzins PA. *Biochim. Biophys. Acta* **1372**, 78–90.
44. Pierre, T.N., Seon, A.A., Amiche, M. & Nicolas, P. (2000) Phylloxin, a novel peptide antibiotic of the dermaseptin family of antimicrobial/opioid peptide precursors. *Eur. J. Biochem.* **267**, 370–378.
45. Combet, C., Blanchet, C., Geourjon, C. & Deleage, G. (2000) NPS@: network protein sequence analysis. *Trends Biochem. Sci.* **3**, 147–150.
46. Millhauser, G.L. (1995) Views of helical peptides: a proposal for the position of 3(10)-helix along the thermodynamic folding pathway. *Biochemistry* **34**, 3873–3877.
47. Sansom, M.S.P. (1993) Alamethicin and related peptaibols-model ion channels. *Eur. Biophys. J.* **22**, 105–124.
48. Cafiso, D.S. (1994) Alamethicin, a peptide model for voltage gating and protein–membrane interactions. *Annu. Rev. Biophys. Biomol. Struct.* **2**, 141–165.
49. Béven, L., Helluin, O., Molle, G., Duclohier, H. & Wróblewski, H. (1999) Correlation between anti-bacterial activity and pore sizes of two classes of voltage-dependent channel-forming peptides. *Biochim. Biophys. Acta* **1421**, 53–63.
50. von Heijne, G. (1983) Patterns of amino acids near signal-sequence cleavage sites. *Eur. J. Biochem.* **133**, 17–21.
51. Zanetti, M., Gennaro, R. & Romeo, D. (1995) Cathelicidins: a novel protein family with a common proregion and a variable C-terminal antimicrobial domain. *FEBS Lett.* **374**, 1–6.
52. Vouille, V., Amiche, M. & Nicolas, P. (1997) Structure of genes for dermaseptins B, antimicrobial peptides from frog skin. *FEBS Lett.* **414**, 27–31.
53. Schiffer, M. & Edmundson, A. (1967) Use of helical wheels to represent the structures of proteins and to identify segments with helical potential. *Biophys. J.* **7**, 121–135.